

# Single Molecule Immunoassay on Plasmonic Platforms

R. Luchowski<sup>1,2,\*</sup>, E.G. Matveeva<sup>1</sup>, T. Shtoyko<sup>3</sup>, P. Sarkar<sup>1</sup>, L.D. Patsenker<sup>4,5</sup>, O.P. Klochko<sup>4</sup>, E.A. Terpetschnig<sup>5,6</sup>, J. Borejdo<sup>1</sup>, I. Akopova<sup>1</sup>, Z. Gryczynski<sup>1,7</sup> and I. Gryczynski<sup>1,7</sup>

<sup>1</sup>Center for Commercialization of Fluorescence Technologies (CCFT), Department of Molecular Biology & Immunology, UNTHSC, Fort Worth, TX 76107, USA; <sup>2</sup>Department of Biophysics, Institute of Physics, Maria Curie-Skłodowska University, 20-031 Lublin, Poland; <sup>3</sup>University of Texas at Tyler, Tyler, TX 75799, USA; <sup>4</sup>SSI "Institute for Single Crystals" of the National Academy of Sciences of Ukraine, 61001 Kharkov, Ukraine, <sup>5</sup>SETA BioMedicals, 2014 Silver Ct East, Urbana, IL 61801 USA; <sup>6</sup>ISS, Inc., 1602 Newton Drive, Champaign, IL 61822, USA; <sup>7</sup>Department of Cell Biology and Anatomy, UNTHSC, Fort Worth, TX 76107, USA

**Abstract:** We examined the photophysical properties of the new near infrared (NIR) fluorescent label SeTau-665 on a plasmonic platform of self-assembled colloidal structures (SACS) of silver prepared on a semitransparent silver film. A SeTau-665 immunoassay was performed on this platform and a control glass slide. The fluorescence properties of this label substantially change due to plasmonic interactions. While the average brightness increase of SeTau 665 in ensemble measurements was about 70-fold, fluorescence enhancements up to four-hundred times were observed on certain "hot spots" for single molecule measurements. The intensity increase is strongly correlated with a simultaneous decrease in fluorescence lifetime in these "hot spots". The large increase in brightness allows the reduction of the excitation power resulting in a reduced background and increased photostability. The remarkable fluorescence enhancements observed for SeTau 665 on our plasmonic platform should allow to substantially improve single molecule detection and to reduce the detection limits in sensing devices.

**Keywords:** Plasmonic platforms, single molecule detection, fluorescence enhancement, fluorescence lifetime imaging microscopy.

## 1. INTRODUCTION

Novel, ultra-sensitive methods and techniques that enable measurements at low fluorophore concentrations are in high demand. The use of powerful excitation sources/pulses is not always an acceptable solution for increasing the sensitivity because of increased photo-damage and background. Metal enhanced fluorescence offers a way to increase brightness and photostability at the same time [1]. The modification of the molecular fluorescence by presence of metallic nanoparticles has been studied already for few decades [2-5], and still is of major interest in many laboratories around the world [6-10]. According to the general understanding, fluorophore-metallic nanoparticle interactions result in a diversity of effects: at a close proximity, below 4-5 nm from the nanoparticles, the fluorescence is strongly quenched [11, 12], and for a long time it was the only observed effect. Relatively recently, it has been shown experimentally that at a distance of 5-20nm fluorescence is enhanced [13, 14]. There are two possible contributions of this effect. First, under the influence of incident light, molecule goes to excited state and interacts with metal. Metal particles accelerate the fluorophore's radiation decay rate and in result enhance the emission. This effect is also known as radiative decay engineering [1]. Under such conditions, a molecular mechanism

of feedback de-excitation is activated, resulting in both, increased photostability and quantum yield with simultaneous decrease of lifetime. The second effect is enhanced local field which acts simultaneously with previous one. Impinging illumination on metallic nanoparticles modifies the electric field around the metallic particles and induces free electron oscillations (localized plasmons) [15-17]. As has been established, the light intensity around the metal particle can be increased about a hundred-fold in comparison to the absence of a particle. The enhanced intensity provides locally a higher excitation rate. The effects also depend on the size and shape of nanoparticles: the observed intensity is not equal at every place of the nanoparticle and therefore has the nature of a local field enhancement [18, 19]. The total fluorescence enhancement is a product of these two effects, RDE and enhanced local field.

A number of promising metal structures which can increase fluorescence signal have been proposed. Silver Island Films which provide about 5-15-fold enhancement [20], fractal-like structures resulted in higher enhancement in "hot spots" [6, 21, 22], and SIFs deposited on silver or gold films with an about 50-fold enhancement [23, 24]. Recently, we found that strong enhancement on a gold film based plasmonic platform may change the shape of the emission spectrum [10].

Here we present unprecedented enhancements, up to 400-fold in "hot spots" on a silver-film based plasmonic platform for the new fluorescence label SeTau-665. Two sets of measurements were used: ensemble and single molecule

\*Address correspondence to this author at the Center for Commercialization of Fluorescence Technologies (CCFT), Department of Molecular Biology & Immunology, UNTHSC, Fort Worth, TX 76107, USA and Department of Biophysics, Institute of Physics, Maria Curie-Skłodowska University, 20-031 Lublin, Poland; E-mail: rluchows@hsc.unt.edu

(SM). The locations of hot spots were measured using a Fluorescence Lifetime Imaging Microscopy set up.

## 2. MATERIALS AND METHODS

### 2.1. Preparation of Self Assembled Colloidal Structures (SACS)

Prior to SACS preparation, the silver colloids were made as previously described [25]. Briefly, all necessary glassware were soaked in a base bath overnight and washed scrupulously with deionized water. The solution of 0.18 mg/mL silver nitrate (200 mL) was heated and stirred in a 250 mL Erlenmeyer flask at 95°C. The first 0.5 mL aliquot of 34 mM trisodium citrate solution was added dropwise. The solution was stirred for 20 min and warmed to 96-98°C. Then five aliquots (0.7 mL each) of 34 mM trisodium citrate were added dropwise to the reaction mixture every 15-20 min. Stirring was continued for 25 min until the milky yellow color remained and the mixture was cooled in an ice bath for 15 min. Then the silver colloids were used to prepare SACS as described earlier [10]. Briefly, slide surfaces were cleaned and drop coated with silver colloids. The slides were air dried to form SACS. The dry slides with self-assembled nanoparticles were stored and used within a month.

### 2.2. Atomic Force Microscopy (AFM) Measurements

AFM images were taken on Explorer Scanning Probe Microscope (ThermoMicroscopes). Samples were imaged showing 8x8µm<sup>2</sup> area with the resolution 300x300 pixels in contact mode. Image data was processed and analyzed on Veeco DI SPMLab software.

### 2.3. Preparation of the SeTau-665 Immunoassay

Reporter anti-rabbit IgG antibodies were labeled with Setau-665 (Setau-665-di-NHS, SETA Biomedicals, Urbana, IL, USA, catalog # K9-4113). An aliquote of a freshly prepared stock solution of the reactive dye (5 mg/mL in DMSO) was added to the solution of IgG antibodies (5 mg/mL) in Na-bicarbonate buffer (0.1 M, pH 8.3) and incubated at room temperature in the dark, stirring gently, for 1 hour. Unconjugated dye was separated from the labeled protein by size-exclusion chromatography using 30,000 MW resin and Na-phosphate buffer (50 mM, pH 7.3) as eluent. The dye/protein ratio in the conjugates was determined spectrophotometrically as described earlier [26]: dye concentration was determined from the visible part of spectra, using a molar extinction coefficient  $\epsilon_{665} = 150,000 \text{ cm}^{-1}\text{M}^{-1}$ . The antibody concentration was determined from the UV part of spectra ( $\epsilon_{280} = 203,000 \text{ cm}^{-1}\text{M}^{-1}$  for IgG), taking into account the UV absorbance contribution from the covalently bound dye. This contribution was determined by measuring absorbance spectra of the free dyes and found to be  $0.19 \times A_{665}$ , where  $A_{665}$  is absorbance at 665 nm, for SeTau-665. Dye/IgG ratio was 0.4.

### 2.4. Model Immunoassay

The model immunoassay was performed on the slide surface as described earlier [27]. Briefly, rabbit IgG was non-covalently immobilized on the sample slide, or goat IgG on the control slide. Slides were covered with 20 µg/mL IgG

solutions in 50 mM Na-phosphate buffer (pH 7.3) and incubated at room temperature overnight. Next, the slides were rinsed with water, and covered with blocking solution (1% bovine serum albumin, 1% sucrose, 0.05% NaN<sub>3</sub>, 0.05% Tween-20 in 50 mM Na-phosphate buffer, pH 7.3) for 2 hours at room temperature. After rinsing with water, Setau-665-labeled anti-rabbit antibody conjugate (20 nM in blocking solution) was added to the sample slides (with rabbit IgG) or control slides (with goat IgG) and after 1 hour incubation and washing, slides were covered with 50 mM Na-phosphate buffer (pH 7.3) and the fluorescence signal was measured.

For SM measurements the assay was performed similarly but the concentration of the SeTau-665 labeled anti-rabbit antibody conjugate was 10 pM.

### 2.5. Steady State Spectroscopy

The emission spectra of the SeTau-665 immunoassay on glass and plasmonic platform (silver SACS surfaces on a silver film) were collected using a Varian Cary 50 spectrophotometer (Varian, Inc.). The samples were placed in a custom-made attachment and excited using front-face geometry at 635nm. Two 665 long wavelength pass filters were placed for observation path.

### 2.6. Photographs

Images were taken with Canon<sup>®</sup> EOS 300 D (Canon Inc.) Digital SLR camera using fixed lens of 50 mm focus, 30 second shutter speed, 11 aperture value and 100 ISO setting. The images were cropped from size 3072 X 2048 pixel to 376 X 343 pixel with Zoombrowser<sup>™</sup> software (Canon Inc. USA) and pasted together with Picasa 3<sup>™</sup> software (Google Inc. USA).

### 2.7. Time Resolved Fluorescence Spectroscopy

Time-domain lifetime measurements of Setau-665 on different substrates were performed using the FluoroTime 200 (FT200) time-resolved spectrofluorometer (PicoQuant GmbH, Berlin, Germany) equipped with a Hamamatsu R3809U-50 microchannel plate photomultiplier detector. A pulsed light-emitting 635nm laser was used for the excitation. The detection was through a monochromator supported with two 665nm long-pass emission filters in order to reject the scattered excitation light. The data was stored and analyzed using FluoFit v. 4.4 software (PicoQuant GmbH). Fluorescence intensity decay curves were deconvoluted with the instrument response function and analyzed as a sum of exponential terms:

$$I(t) = \sum_i \alpha_i \exp(-t/\tau_i) \quad (1)$$

where  $I(t)$  is the fluorescence intensity at time  $t$  and  $\alpha_i$  is a pre-exponential factor representing the fractional contribution to the time-resolved decay of the component with a lifetime  $\tau_i$  ( $\sum \alpha_i = 1$ ).

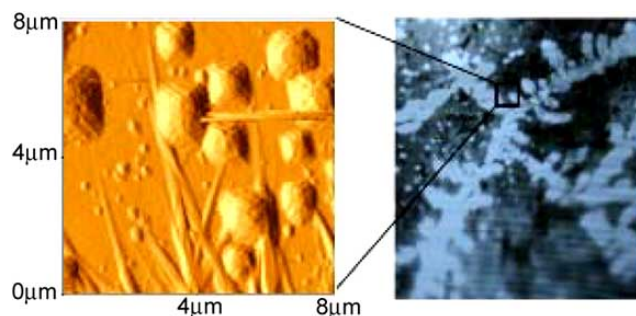
### 2.8. Time Resolved Fluorescence Microscopy

MicroTime200 (Picoquant, GmbH) confocal microscopy system in combination with time-correlated single photon

counting detector (Perkin Elmer avalanche photodiode – APD SPCM-AQR-14) and Olympus IX17 microscope was used. This setting offers spatial and temporal measurements with a high resolution. The 635nm laser light was transferred by single mode fiber to main optical unit with repetition of 20MHz and focused on sample using an Olympus 60x magnification, numerical aperture of 1.2, water immersion objective. Light triggering was accomplished by a PDL828 driver. The sample with dye-immunoassay was placed upside down on a non-fluorescent Menzel-Glaser #1 cover-slip. Focused beam excited sample and fluorescence was collected by the same microscope objective. To remove scattered light, system of razor edge filters was placed on: 650nm long-pass, 640nm long-pass (Semrock) and 665 glass long-pass filters were used. 80nW light intensity was used for gathering data for ensemble and SM imaging. Data was processed by the Pico-Harp300 TCSPC module which gathered information about each detected photon, timing pulse and the number of the APD-channels.

### 3. RESULTS

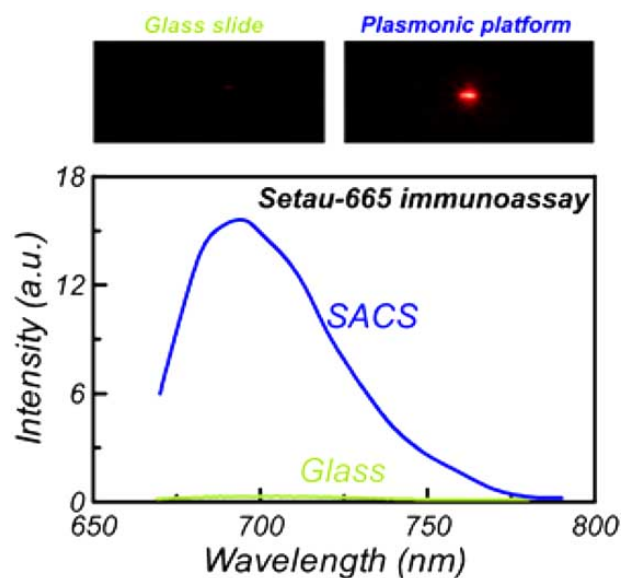
In order to examine the organization of the SACS on the mirror substrate, we have applied the atomic force microscopy (AFM) imaging technique. Scheme 1 presents a typical AFM image of the  $8 \times 8 \mu\text{m}^2$  fragment. The inhomogeneous diversity of structures corresponds to self assembled silver organization. As can be seen, the majority of SACS create  $\sim 2 \mu\text{m}$  diameter silver aggregates. The expectation is that heterogeneity of silver organization impact on non-uniform fluorescence enhancement.



**Scheme 1.** (left) AFM image of SACS, (right) morphology photograph of SACS taken from AFM monitor.

#### 3.1. Ensemble Approach

Fig. (1) shows the ensemble (high concentration of the dye) emission spectra of SeTau-665 on the plasmonic platform (blue line) and the glass (light green) surfaces. A considerably stronger emission was found for SeTau 665 deposited on the metallic structures. SeTau-665 has a strong emission peak around 690nm on glass and exhibits a slight red shift of its emission maximum to 695nm on the plasmonic platform. This indicates strong interactions between the metallic surface and the dye as already reported earlier [10, 28]. In order to estimate the degree of enhancement the integrated fluorescence intensity of the SeTau-665 molecules on the plasmonic platform was compared to that on the glass, resulting in  $\sim 70$ -fold enhancement factor. The intensity from wavelength 675nm to 750nm was integrated for the analysis.



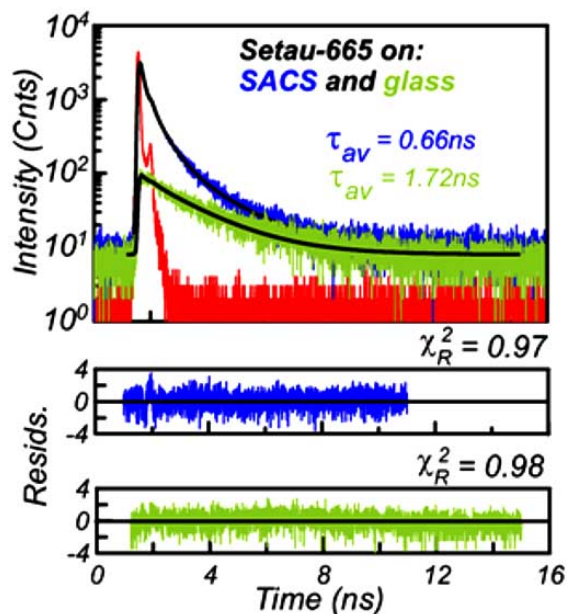
**Fig. (1).** Emission spectra of SeTau-665 immunoassay (ensemble concentration) on glass and SACS surfaces. Top panels show photographs taken with 635nm excitation and observed through 695nm long wave pass filter

Fig. (2) displays typical decay profiles of fluorescence intensity for molecules assembled on the glass and platform. The decay data were fitted to a multi-exponential model. The bottom panels show deviations from the models and goodness of the fit values. The parameters of fluorescence lifetimes are shown in Table 1. As seen from the table, fluorescence decays could be fitted well with a bi-exponential function for glass and tri-exponential one for the platform. The mean fluorescence lifetime of SeTau-665 on the platform is decreased to 0.66ns due to an increase in the radiative decay rate of the fluorophore near the metallic surface. It is clear (see Table 1) that on the plasmonic platform one of lifetime component (1.82 ns) with amplitude 0.22 represents a fraction of the dye not interacting with Ag-SACS.

We also applied confocal microscopy measurements in order to get fluorescence intensities which are shown in Fig. (3) The left and right images were taken from different samples prepared separately. Fig. (3) bottom was plotted as functions of the intensity and lifetime versus the position along the arrows depicted on the images of the above plots. As expected, the mean fluorescence intensity on SACS substrates is much stronger than on glass but interestingly one can also observe intensity “hot spots” on plasmonic platforms. They are easily identified with the correlation of two parameters: the intensity jump corresponds to a decrease of the lifetime parameter. A few examples of such correlated changes of intensity and lifetime are indicated in position by vertical black dotted lines. It is also important to note that no “hot spots” were observed on the glass reference slides.

Next, the samples were investigated for their photostability. Fig. (4) shows fluorescence intensity traces taken by microscope objective focused in one point of the sample. The excitation power was adjusted to yield the same inten-

sity at time zero. For dye deposited on the platform we noticed increased photostability (blue line) in comparison to the same concentration of the dye deposited on glass (light green).



**Fig. (2).** Results of iterative time domain reconvolution analysis of intensity decays of SeTau-665 immunoassay deposited on glass and SACS. Instrument response function obtained at 635nm using Lu-dox scatterer.

### 3.2. Single Molecule Detection Approach

The advantage of applying SACS structures deposited on silver mirrors for fluorescence detection of small concentrations of the dye can be also clearly seen from Fig. (5). This figure presents  $20 \times 20 \mu\text{m}^2$  images of picomolar concentrations of Setau-665 IgGs deposited on glass and SACS. Parts: A and B of Fig. (5) were obtained with the same (80nW) intensity of excitation light for glass and SACS, respectively. With such small excitation intensity SMD can be measured only on SACS structures. For seeing SM on glass an 80-times higher laser power is required (data presented on Fig. (5C)). The significance of this observation indicates the possibility of applying low intensity laser light for monitoring SM.

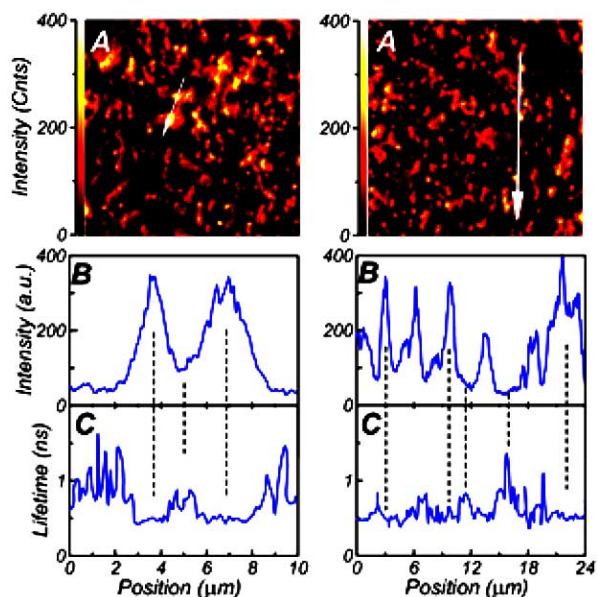


**Fig. (3).**  $30 \times 30 \mu\text{m}^2$  scanning confocal images of SeTau-665 on self-assembled silver colloids (SACS) with lifetime (C) and intensity (B) traces versus position pointed along the arrows on the intensity image (A). The images on the left and right parts of figure were taken from independently prepared high density immunoassays.

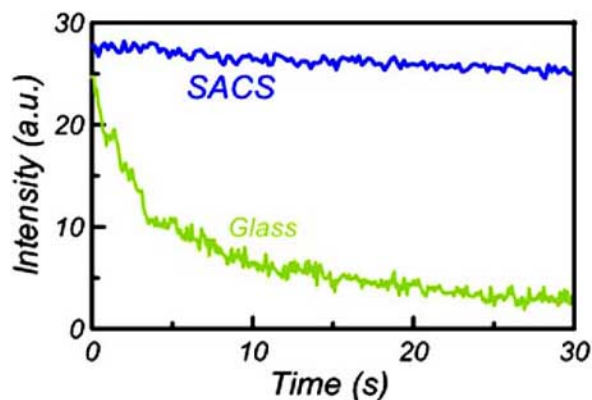


**Fig. (4).** The stability of SeTau-665 immunoassay on self-assembled colloidal structures (dark) and glass (light) under constant laser illumination in the confocal fluorescence lifetime microscope.

**Table 1.** Multiexponential Analysis of SeTau-665 Depositions on Different Substrates. The Excitation was 635nm. The Observation was 690 nm for a Glass and 695 nm for Plasmonic Platform

Substrate	$\alpha_1$	$\tau_1$ (ns)	$\alpha_2$	$\tau_2$ (ns)	$\alpha_3$	$\tau_3$ (ns)	$\bar{\tau}$ (ns)	$\langle \tau \rangle$ (ns)	$\chi^2$
Glass	0.06	0.24	0.94	1.82			1.72 <sup>a</sup>	1.3 <sup>b</sup>	0.98
SACS	0.37	0.11	0.41	0.5	0.22	1.82	0.66	0.24	0.97

$${}^a \bar{\tau} = \sum_i f_i \tau_i, \quad f_i = \frac{\alpha_i \tau_i}{\sum_i \alpha_i \tau_i}$$

$${}^b \langle \tau \rangle = \sum_i \alpha_i \tau_i$$

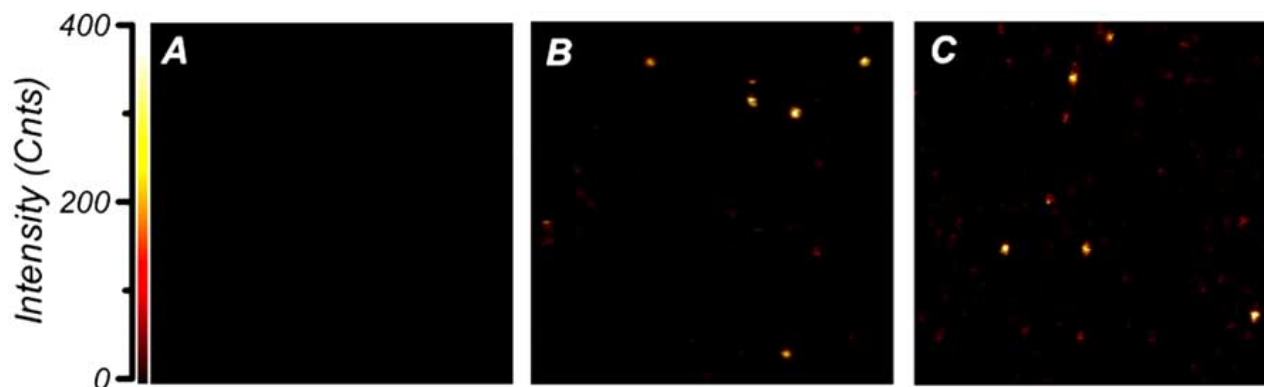


**Fig. (5).** 20x20  $\mu\text{m}^2$  confocal fluorescence lifetime images of SeTau-665 in SM concentration regime using 635nm solid state laser. **A)** image taken for the dye on glass with 80nW laser power; **B)** image taken for the dye deposited on SACS with 80nW laser power; **C)** image taken for the dye deposited on glass with 1.6 $\mu\text{W}$  laser power.

Fig. (6) presents the typical examples of time courses of SM of Setau-665 from bright spots presented on Fig. (5). Data were taken for dye on a glass (top panels) and the plasmonic platform (bottom panels). Both sets of time courses show the same principal step-wise drops of the fluorescence intensity, characteristic for photobleaching effects of SM [29-31]. Importantly, Setau-665 shows a huge disproportion of the length of time course depending on the sample deposition. Clearly, at first approximation the SM deposition on SACS results in higher survival time for molecules. This can be clearly seen statistically from histograms presented in Fig. (7), where the numbers of courses were plotted against the survival time. The majority of molecules deposited on glass undergo fast photobleaching during the first 10s, whereas on SACS we observed two maxima of distribution. One, which is located in the first 10s and a second one, that can be found at 100-110s. We believe that first maximum arises from molecules which were not deposited on SACS but simply on silver glass, outside the enhancement region. The position of the second maximum provides experimental prove of increased photostability for molecules deposited on SACS. In turn, this observation allows for longer molecule observation and longer monitoring of any processes undergoing during this time. On the plasmonic platform the reduced lifetime prevents photodegradation, which occurs in the excited state. Furthermore, from the time courses we calculated the number of photons observed until total photobleaching of the molecule. The results are presented on Fig. (8). The parameter named "Number of emitted photons" is directly related to the stability and brightness of the molecule. Again we observed a very homogenous Gaussian statistic for SeTau 665 on glass (Fig. (8A)) and heterogeneous distribution for the SACS substrates. The reason seems to be the same as above: a part of the molecules was not deposited on SACS. These histograms provide real numbers of photons revealing that SACS substrates provide more than 100-fold better conditions for brightness than glass as calculated from integration of histograms. We would like to emphasize that all the measurements were performed under ambient conditions without applying any deoxygenates.

#### 4. CONCLUSIONS

The studies presented here clearly demonstrate that self-assembled silver colloidal nanostructures on a metallic film

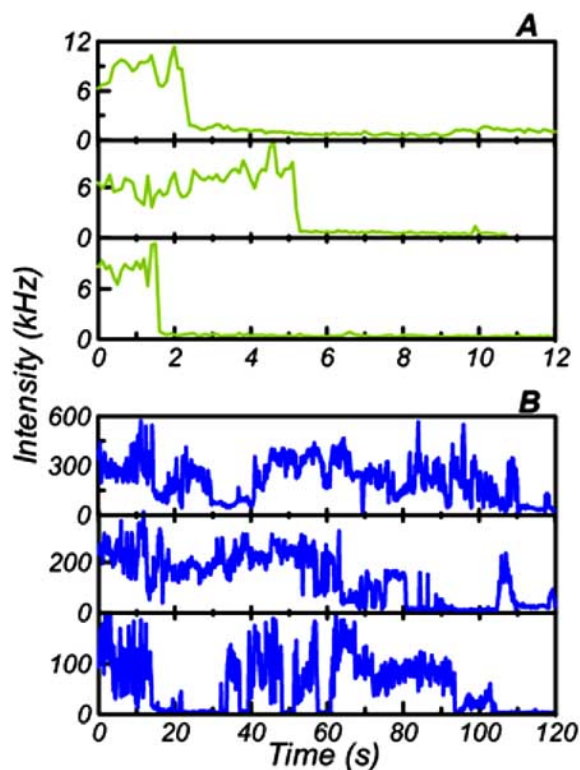


**Fig. (6).** Representative time traces of single SeTau-665 molecules immobilized on glass **(A)** and SACS **(B)**.

result in an efficient plasmonic platform capable of significantly enhancing the fluorescence emission. The brightness and lifetime of the dye on the plasmonic platform strongly correlate - the strongest enhancement corresponds to the shortest lifetime. For high density immunoassays we recorded an about 70-fold average enhancement. This suggests that for fluorescence sensing one can reduce the excitation power many-fold thereby decreasing the unwanted background and/or the use alternative excitation sources like light emitting diodes (LEDs).

Interestingly, with plasmonic platforms we observed also "hot spots", where the recorded emission enhancement of SeTau 665 was about 400-fold which according to our knowledge was not previously reported in the literature. The

SMD measurements on plasmonic platforms can be done with extremely low excitation power which reduces the background fluorescence and blinking from silver nanoparticles. We believe that many SM studies which were impossible previously can be successfully performed on such plasmonic platforms based on SeTau 665.

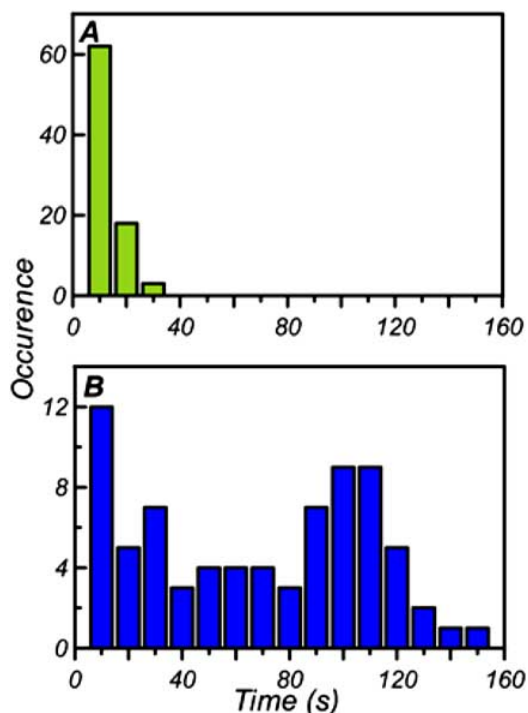


**Fig. (7).** Histograms of “survival time” of single SeTau-665 molecules on (A) glass and (B) SACS. The histograms were built from about 150 SM courses for glass and SACS.

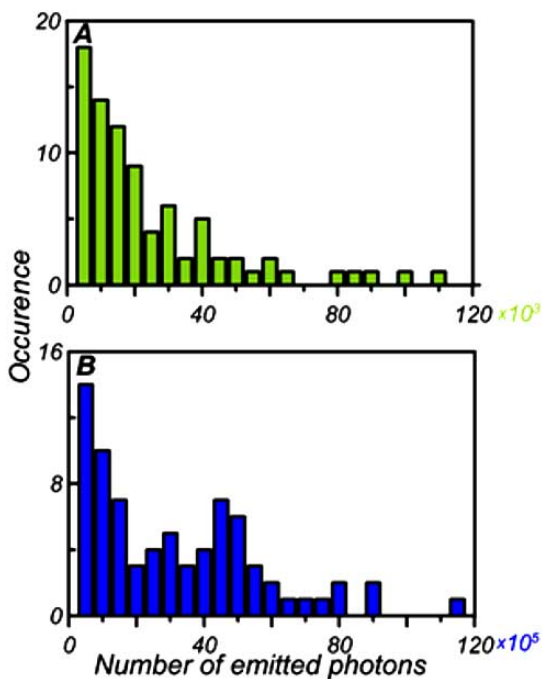


**Fig. (8).** Histograms of total number of photons gathered before photobleaching for SeTau-665 immobilized on (A) glass and (B) SACS.

Interestingly, we can see close correlation of stability behavior measured in ensemble as well as SM level. Our studies indicate that plasmonic surfaces can influence the photophysical properties of even SM.

## ACKNOWLEDGEMENTS

This work was supported by NIH grants R41EB008614, R43CA132547 and by ARPATP Project 000130-0042-2007 (IG). T.S. was supported by Research Corporation for Science Advancement and the Welch Foundation (BP-0037). Rafal Luchowski is a recipient of a researcher’s mobility program from the Polish Ministry of Science and Higher Education.

## REFERENCES

- [1] Lakowicz, J.R. Metal-enhanced fluorescence, Chapter 25. In: *Principles of Fluorescence Spectroscopy, Radiative Decay Engineering*; 3<sup>rd</sup> ed. Springer: New York, NY, USA, **2006**, pp. 841-59.
- [2] Das, P.; Metiu H. Enhancement of molecular fluorescence and photochemistry by small metal particles. *J. Phys. Chem.*, **1985**, *89*, 4680-4687.
- [3] Drexhage, K.H. Influence of a dielectric interface on fluorescence decay time. *J. Lumin.*, **1970**, *1*(2), 693-701.
- [4] Ritchie, G.; Burstein E. Luminescence of dye molecules adsorbed at a Ag surface. *Phys. Rev. B*, **1981**, *24*(8), 4843-4846.
- [5] Weitz, D.A.; Garoff, S. The enhancement of Raman scattering, resonance Raman scattering, and fluorescence from molecules adsorbed on a rough silver surface. *J. Chem. Phys.*, **1983**, *78*(9), 5324-5338.
- [6] Goldys, E.M.; Drozdowicz-Tomsia, K.; Xie, F.; Shtoyko, T.; Matveeva, E.; Gryczynski, I.; Gryczynski, Z. Fluorescence amplification by electrochemically deposited silver nanowires with fractal architecture. *J. Am. Chem. Soc.*, **2007**, *129*(40), 12117-12122.
- [7] Ritman-Meer, T.; Cade, N.I.; Richards, D. Spatial imaging of modifications to fluorescence lifetime and intensity by individual Ag nanoparticles. *Appl. Phys. Lett.*, **2007**, *91*, 123122.
- [8] Seelig, J.; Leslie, K.; Renn, A.; Kühn, S.; Jacobsen, V.; van de Corput, M.; Wyman, C.; Sandoghdar, V. Nanoparticle-induced fluorescence lifetime modification as nanoscopic ruler: Demonstration at the single molecule level. *Nano Lett.*, **2007**, *7*(3), 685-689.
- [9] Szmajda, H.; Ray, K.; Lakowicz, J.R. Metal-enhanced fluorescence of tryptophan residues in proteins: Application toward label-free bioassays. *Anal. Biochem.*, **2009**, *385*(2), 358-364.
- [10] Sørensen, T.J.; Laursen, B.W.; Luchowski, R.; Shtoyko, T.; Akopova, I.; Gryczynski, Z.; Gryczynski, I. Enhanced fluorescence emission of Me-ADOTA(+) by self-assembled silver nanoparticles on a gold film. *Chem. Phys. Lett.*, **2009**, *476*(1-3), pp. 46-50.
- [11] Axelrod, D.; Hellen, E.H.; Fulbright, R.M. Biochemical applications. Lakowicz, J.R., Ed.: In: *Topics in Fluorescence Spectroscopy*, Plenum Press: New York **1992**, Vol. 3, pp. 289-343.
- [12] Barnes, W.L. Fluorescence near interfaces: The role of photonic mode density. *J. Mod. Opt.*, **1998**, *45*, 661-699.
- [13] Malicka, J.; Gryczynski, I.; Gryczynski, Z.; Lakowicz, J.R. Effects of fluorophore-to-silver distance on the emission of cyanine-dye-labeled oligonucleotides. *Anal. Biochem.*, **2003**, *315*(1), 57-66.
- [14] Sokolov, K.; Chumanov, G.; Cotton, T.M. Enhancement of molecular fluorescence near the surface of colloidal metal films. *Anal. Chem.*, **1998**, *70*(18), 3898-3905.
- [15] Fu, Y.; Lakowicz, J.R. Modification of single molecule fluorescence near metallic nanostructures. *Laser Photon Rev.*, **2009**, *3*, 221-233.
- [16] Lakowicz, J.R. Radiative decay engineering: biophysics and biomedical applications. *Anal. Biochem.*, **2001**, *298*, 1-24.
- [17] Lakowicz, J.R.; Shen, Y.; D’Auria, S.; Malicka, J.; Fang, J.; Gryczynski, Z.; Gryczynski, I. Radiative decay engineering. 2. Effects of Silver Island films on fluorescence intensity, lifetimes, and resonance energy transfer. *Anal. Biochem.*, **2002**, *301*(2), 261-277.
- [18] Hao, E.; Schatz, G.C. Electromagnetic fields around silver nanoparticles and dimmers. *J. Chem. Phys.*, **2004**, *120*(1), 357-366.

- [19] Kelly, K.L.; Coronado, E.; Zhao, L.L.; Schatz, G.C. The optical properties of metal nanoparticles: The influence of size, shape, and dielectric environment. *J. Phys. Chem. B*, **2003**, *107*, 668-677.
- [20] Lukomska J.; Malicka, J.; Gryczynski, I.; Lakowicz, J.R. Photostability of Cy3 and Cy5-labeled DNA in the presence of metallic silver particles. *J. Fluoresc.*, **2004**, *14*(4), 417-423.
- [21] Parfenov, A.; Gryczynski, I.; Malicka, J.; Geddes, C.D.; Lakowicz, J.R. Enhanced fluorescence from fluorophores on fractal silver surfaces. *J. Phys. Chem. B*, **2003**, *107*(34), 8829-8833.
- [22] Shtoyko, T.; Matveeva, E.G.; Chang, I.F.; Gryczynski, Z.; Goldys, E.; Gryczynski, I. Enhanced fluorescent immunoassays on silver fractal-like structures. *Anal. Chem.*, **2008**, *80*(6), 1962-1966.
- [23] Barnett, A.; Matveeva, E.G.; Gryczynski, I.; Gryczynski, Z.; Goldys E.M. Coupled plasmon effects for the enhancement of fluorescent immunoassays. *Physica. B, Condens. matter*, **2007**, *394*, 297-300.
- [24] Matveeva, E.G.; Gryczynski, I.; Barnett, A.; Leonenko, Z.; Lakowicz, J.R.; Gryczynski, Z. Metal particle-enhanced fluorescent immunoassays on metal mirrors. *Anal. Biochem.*, **2007**, *363*(2), 239-245.
- [25] Lukomska, J.; Gryczynski, I.; Malicka, J.; Makowiec, S.; Lakowicz, J.R.; Gryczynski, Z. One- and two-photon induced fluorescence of pacific blue-labeled human serum albumin deposited on different core size silver colloids. *Biopolymers*, **2006**, *81*, 249-255.
- [26] Haugland, R.P. Coupling of monoclonal antibodies with fluorophores. *Meth. Mol. Biol.*, **1995**, *45*, 205-221.
- [27] Matveeva, E.G.; Gryczynski, Z.; Malicka, J.; Gryczynski, I.; Lakowicz, J.R. Metal-enhanced fluorescence immunoassays using total internal reflection and silver island-coated surfaces. *Anal. Biochem.*, **2004**, *334*(2), 303-311.
- [28] Chizhik, A.; Schleifenbaum, F.; Gutbrod, R.; Chizhik, A.; Khoptyar, D.; Meixner, A.J.; Enderlein, J. Tuning the fluorescence emission spectra of a single molecule with a variable optical sub-wavelength metal microcavity. *J. Phys. Rev. Lett.*, **2009**, *102*(7), 073002.
- [29] Ha, T.; Ting, A.Y.; Liang, J.; Deniz, A.A.; Chemla, D.S.; Schultz, P.G.; Weiss, S. Temporal fluctuations of fluorescence resonance energy transfer between two dyes conjugated to a single protein. *Chem. Phys.*, **1999**, *247*(1), 107-118.
- [30] Weber, M.A.; Stracke, F.; Meixner, A.J. Dynamics of single dye molecules observed by confocal imaging and spectroscopy. *Cytometry*, **1999**, *36*(3), 217-223.
- [31] Zhang, J.; Fu, Y.; Chowdhury, M.H.; Lakowicz, J.R. Single-molecule studies on fluorescently labeled silver particles: Effects of particle size. *J. Phys. Chem. C*, **2008**, *112*(1), 18-26.

---

Received: August 12, 2009

Accepted: September 01, 2009